Structure-property relationship of sol-gel synthesised zinc-oxide nanoparticles

N V Peterson[1], C J Arendse[1], K T Hillie[2] and M Dhlamini[3]

[1]Department of Physics, University of the Western Cape, Private Bag X17, Bellville 7535, South Africa,

[2]DST/CSIR National Centre for Nano-Structured Materials, P. O. Box 395, Pretoria 0001, South Africa,

[3]Department of Physics, University of South Africa, P. O. Box 392, Muckleneuk Ridge UNISA 0003, South Africa

Abstract. Zinc-oxide nanoparticles are well known for their novel optical and electronic properties for applications in various fields such as solar cells, ultra violet shielding, gas sensors, paint and heat mirrors. We report on the relation between the structure and optical properties of ZnO nanoparticles synthesized via the sol-gel technique, with specific emphasis on the effect of growth and reaction temperatures. High-resolution microscopy techniques, complemented by x-ray diffraction, confirm that the crystallinity and particle size of ZnO nanoparticles is directly related to the synthesis conditions. Optical absorption and emission spectroscopy show that optical band gap and photoluminescence of the ZnO nanoparticles are intimately related to its structural properties, ascribed to the quantum confinement effect. Photoluminescence spectroscopy confirm the emission peaks in the ultraviolet (380 nm) and visible (500 nm) region; the latter attributed to the presence of the singly ionized oxygen vacancies in the nanoparticle.

1. Introduction

ZnO is an important II-VI compound semiconductor with a wide direct band (3.37 eV) and a large excitation binding energy (60 meV) at room temperature [1 – 5]. Room temperature photoluminescence of ZnO typically exhibits dual emissions in the near UV and visible range. The UV near band edge emission is at approximately 370 nm, which is a broad UV emission that is sharp and highly intense. The other visible emission is in the range from 450 – 730 nm [6, 7] and it is relatively weak and broad. The broad emission is due to the existence of surface defects and the band edge emissions are found to be more stable for most of the II-IV semiconductors [7].

ZnO is widely used in various applications such as UV- photodetectors, bulk acoustic wave resonators, gas sensors, solar cells, laser diodes and optical waveguides [8 – 10]. There are several methods reported for the synthesis of ZnO nanoparticles, which include chemical vapor deposition [11], gas-phase method [12], spray pyrolysis, hydrothermal synthesis, micro emulsion, electrochemical method [13], pulsed laser deposition, microwave synthesis and the sol gel method [14, 15]. Recently, a variety of morphologies, including thin films, nanospheres, nanorods, nanowires, nanobelts, nanotubes, nanoflowers and nanowhiskers [16 – 20], have been prepared by some of the methods above. ZnO nanoparticles are

receiving worldwide interest because of the novel optical and electrical properties for various applications [21]. ZnO nanoparticles, produced by the sol gel method, show excellent optical properties in which good control of the size and morphology of the particles is achieved. This method costs is very low and it is reliable, repeatable and simple [4].

In this paper, the sol gel method is used to synthesis ZnO nanoparticles. Investigations of the effect of growth temperature and reaction temperature on the particles size, the morphology, crystallinity, and optical emission and absorption properties were carried out by using x-ray diffraction, transmission electron microscopy, photoluminescence spectroscopy and ultraviolet-visible spectroscopy.

2. Experiment

All chemicals were purchased from the supplier and were used without further purification. In the typical synthesis, 0.46g of zinc acetate (Zn $(CH_3CO_2)_2$) was dissolved in 30ml of ethanol (CH_3CH_2OH) under vigorous stirring at a temperature of 75 – 80°C for 1 hour. 0.22g of sodium hydroxide (NaOH) was dissolved in 10 ml of CH_3CH_2OH in the ultrasonic bath. Both clear solutions were placed in a water bath with respective temperature in the range 0 – 60^0C for 15 minutes. This temperature is hereafter referred to as the *reaction temperature*. The NaOH solution was added dropwise to the Zn $(CH_3CO_2)_2$ solution under vigorous stirring at temperatures from 0 – 60^0C. This temperature is hereafter referred to as the *growth temperature*. The solution was stirred for an extra 30 minutes. The solution was stored for 24 hours. Purification for the as-prepared ZnO nanoparticles was firstly washed in ethanol. Heptane ($CH_3C_5H_{10}CH_3$) was further added to wash the ZnO nanoparticles. White ZnO nanoparticles precipitated after centrifugation at 4000 rmp for 15 minutes and the unwanted ions were removed. The ZnO precipitate was redispersed in heptane using the ultrasonic bath. The above procedure of washing the ZnO nanoparticles in heptane was repeated three times. The ZnO precipitate was suspended in ethanol and it was dried in the oven at a temperature of 90^0C for 2 hours [22]. Thereafter the required analytical techniques were performed.

The crystallinity and the particles sizes of the ZnO nanoparticles were measured in reflection geometry of the PANalytical X'pert pro PW3040/60 X-Ray diffractometer. The system was operated with a CuKα (λ = 1.54060 Å) monochromatic radiation source at voltage 45.0 kV and the current at 40.0 mA. The XRD pattern was collected in the step scan mode with 2θ-values ranging from 10.0 to 120.0° with a step size of 0.026°. The internal structure, particle size and crystallinity of the ZnO nanoparticles were recorded on a JEOL 2100 high-resolution transmission electron microscopy (HR-TEM) operated at 200 kV accelerating voltage. The optical transmission spectra of ZnO nanoparticles were recorded using the Perkin-Elmer LAMDA 750S UV-VIS spectrophotometer in the range from 200 – 800 nm with a spectral resolution of 1 nm. The emission properties were performed using a Perkin-Elmer LS2 Fluorescence Spectrometer in the range from 340 – 800 with an excitation source of 320 nm.

3. Results and Discussions

3.1. Structural Properties

The XRD patterns of the ZnO nanoparticles synthesized at different reaction and growth temperatures are shown in figure 1. Several preferential orientations in the <100>, <002>, <101>, <102>, <110>, <103>, <112> and <202> directions are observed, which match well with the hexagonal wurtzite structure of ZnO, corresponding with Joint Committee for Powder Diffraction Standards (JCPDS) File no. 36- 1451 [23]. No other diffraction peaks for the reagents are observed, illustrating the enhanced purity of the ZnO nanoparticles. The (101) diffraction peak appears to be dominant in all spectra, implying that the majority of crystallites have a preferred growth along the (101) plane. After quantitative analysis of the (101) diffraction peak, the interplanar spacing (*d*), lattice constants (*a* and *c*) and particle size were calculated for all spectra (not shown). From figure 1, it is clear that with increasing temperature the diffraction peaks

become sharper and stronger, which imply that the crystallinity of the nanoparticles improves. The results show a systematic increase in the particle size with an increase in both the reaction and growth temperature from 3.6 – 4.9 nm and 3.5 – 4.0 nm, respectively. The *d*-spacing, and hence the lattice constants, remains relatively constant as both the reaction and growth temperature increases. However, *a* and *c* deviates from the standard reported values of 3.2475 - 3.2501 Å and 5.2042 - 5.2075 Å, respectively, and the ratio *c/a* varies in the range 1.593 - 1.6035 [24 - 26]. The ratio *c/a* relates the electronegativities of the zinc and oxygen constituents and the components undergoing a massive difference show large departure from the ideal ratio [24].

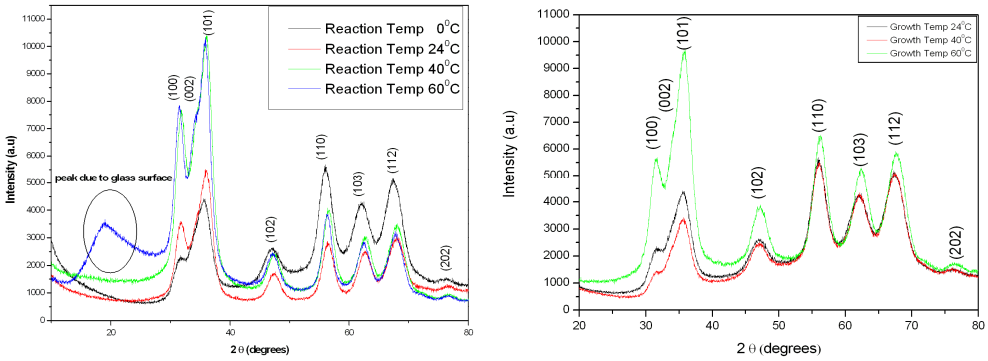

Figure 1. XRD spectra of ZnO nanoparticles synthesized at different reaction and growth temperatures

The crystalline nature and the internal structure of the nanoparticles have been further investigated by HR-TEM. Figures 2 and 3 depict the respective HR-TEM images of the ZnO nanoparticles synthesized at different reaction and growth temperatures, respectively. Clear lattice fringes are present for all samples, indicative of the superior crystallinity. The particle size was statistically measured from the low magnification TEM micrographs (not shown). As in the case for XRD, a growth in the particle size from 4.1 – 6.3 nm and 4.1 – 5.7 nm is observed with an increase in growth and reaction temperature, respectively.

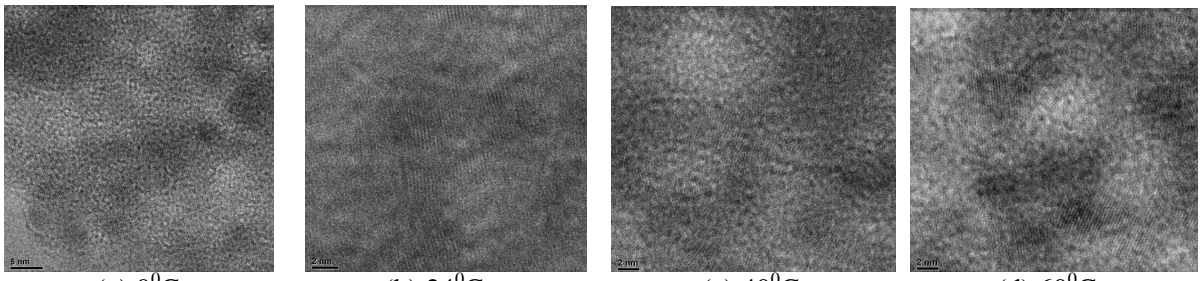

(a) 0^0C (b) 24^0C (c) 40^0C (d) 60^0C

Figure 2. TEM images of ZnO nanoparticles at their respective reaction temperatures at high magnification

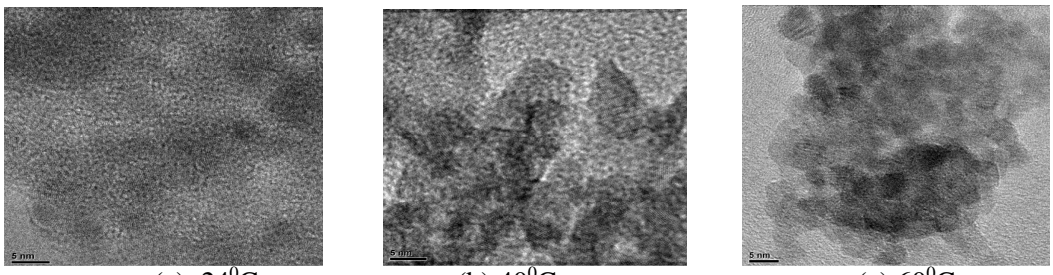

(a) 24^0C (b) 40^0C (c) 60^0C

Figure 3. TEM images of ZnO nanoparticles at their respective growth temperatures at high magnification

3.2. Optical Properties

Figure 4 shows the optical absorbance spectra of ZnO nanoparticles synthesized at the respective reaction and growth temperatures. For qualitative analysis, the optical absorption edge can be estimated from the absorption peak centered around 320 nm. A systematic red shift in the absorption edge is observed with an increase in the reaction and growth temperature, indicative of a reduction in the optical band gap. The reduction in the optical band gap is attributed to a growth in the particle size and is explained by the quantum confinement effect [27].

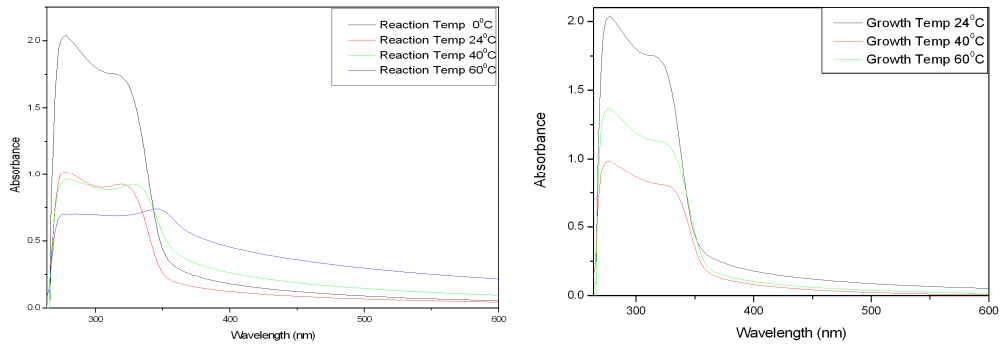

Figure 4. Optical absorption spectra of ZnO nanoparticles synthesized at their respective reaction and growth temperatures.

Figure 5 shows the optical emission (photoluminescence) spectra of ZnO nanoparticles synthesized at the respective reaction and growth temperatures. Two emission peaks are present in the spectrum: one consisting of ultraviolet peak located in the range from 375 – 396 nm, related to the near band gap transition of ZnO which comes from the recombination of free excitons [28]. The other peak is located in the visible emission in the range from 492 – 507 nm, representing the green emission due to the presence of the singly ionized oxygen vacancies. This is caused by the radiative recombination of a photo-generated hole with an electron occupying the oxygen vacancy.

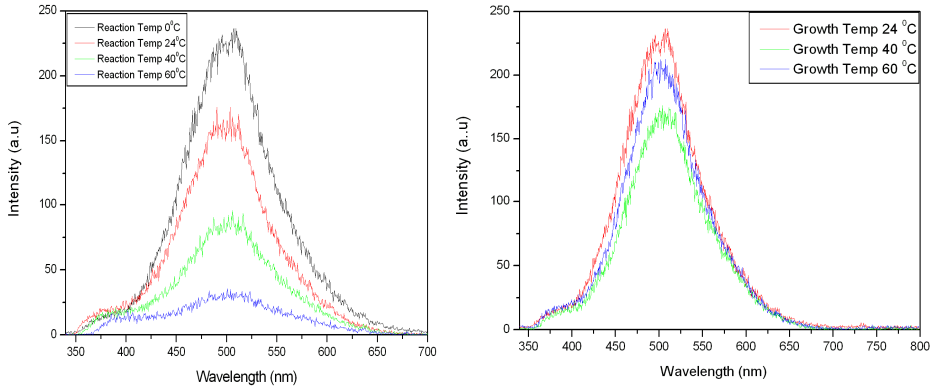

Figure 5. Optical emission (PL) spectra of ZnO nanoparticles synthesized at their respective reaction and growth temperatures.

The intensity of the visible emission band is higher than the ultraviolet emission band for all respective temperatures. A reduction in the intensity of the green emission peak is observed with an increase in the reaction and growth temperature, with the exception of the particles synthesized at a growth temperature of 60 °C. Dijken *et al* [28] reported that the key features of the visible emission process are a very fast trapping of a photogenerated hole at the surface site. It further continues to tunnel the surface trapped hole back into the bulk of the particle to the V^{*}_{o} oxygen vacancy and creates a V^{**}_{o} center where it recombines with a shallowly trapped electron to give rise to a trap emission. As the particle sizes increases the tunneling rate of the surface trapped holes to the V^{**}_{o} center decreases, resulting in the observed reduction in the intensity of the visible emission [28].

4. Conclusion

XRD and HR-TEM show that an increase in reaction and growth temperature results in a growth in the ZnO nanoparticle size with minimum effect on the crystalline structure, i.e. interplanar spacing and lattice constants. Optical absorption spectroscopy show an expected red shift in the absorption edge with an increase in particle size, which is attributed to the quantum confinement effect. Emission spectroscopy show a reduction in the visible emission intensity, which has been related to a growth in the particle size.

5. References

[1] Peng W Q, Qu S C, Cong G W and Wang Z G 2006 *Mater. Sci. Semic. Proc.* **9** 156 - 159
[2] Yu Q, Fu W, Yu C, Yang H, Wei R, Sui Y, Lui Y, Lui Z, Li M, Wang G, Shao C, Lui Y and Zou G 2007 *J. Phys. D: Appl. Phy.* **40** 5592 - 5597
[3] Pal U, Serrano J G, Santiago P, Xiong G, Ucer K B and Williams R T 2006 *Opt. Mater.* **29** 65-69
[4] Vafaee M and Sasani Ghamsari M 2007 *Mater. Lett.* **61** 3265 - 3268
[5] Wu L, Wu Y and Lü W 2005 *Physica.* **28** 76 - 82
[6] Bera D, Qian L, Sabui S, Santra S and Holloway P H 2008 *Opt. Mat.* **30** 1233– 1239
[7] Wang Z G, Zu X T, Zhu S and Wang L M 2006 *Phy. E.* **35** 199–202
[8] Ni Y, Cao X, Wu G, Hu G, Yang Z and Wei X 2007 *Nanotechn.* **18** 155603 – 155609
[9] Baruah S and Dutta J 2009 *Sci. Technol. Adv. Mater.* **10** 45 - 48
[10] Wang L and Muhammed M 1999 *J. Mater. Chem.* **9** 2871 – 2878
[11] Jitianu M and Goia D V 2007 *J. Coll. Interf, Sci*. **309** 27 - 85
[12] Zhou J, Zhao F, Wang Y, Zhang Y and Yang L 2007 *J. Lumin.* **122 – 123** 195
[13] Zhang Y L, Yang Y, Zhao J H, Tan R Q, Cui P and Song W J 2009 *J. Sol-Gel Sci Technol.* **51** 198
[14] Sridevi D and Rajendran K V 2009 *Int. J. Nanotechn. Appl.* **3(2)** 43
[15] Bouvy C, Marine W, Sporken R and Su B L 2006 *Chem. Phys. Lett.* **428** 312

[16] Gumus C, Ozkendir O M, Kavak H and Ufuktepe Y 2006 *J. Optoel. Adv. Mater.* **8** 299 – 303
[17] Seow Z L S, Wong A S W, Thavasi V, Jose R, Ramakrishna S and Ho G W 2009 *Nanotech.* **20** 045604 - 045610
[18] Xia Y , Yang P, Sun Y, Wu Y , Mayers B, Gates B, Yin Y, Kim F and Yan H 2003 *Adv. Mater.* **15** 353 – 389
[19] Kharisov B I 2008 *Rec.Pat. Nanotech.* **2** 190 - 200
[20] Hu X, Masuda Y, Ohji T and Kato K 2008 *J. Cer. Soc. Japan.* **116** 384 - 388
[21] Yang J, Liu X, Yang L, Wang Y, Zhang Y, Lang J, Gao M and Wei M 2009 *J. Alloys & Comp.* ***485*** 743 - 746
[22] Dhlamini M S 2008 PhD Dissertation (University of Free State)
[23] Shen L, Bao N, Yanagisawa K, Domen K, Gupta A and Grimes C A 2006 *Nanotech.* **17** 5117
[24] Özgür Ü, Alivov Ya I, Liu C, Teke A, Reshchikov M A, Doğan S, Avrutin V, Cho S J and Morkoç H 2005 *J. Appl. Phy.* **98** 041301
[25] Morkoç H and Özgür Ü 2009 *Zinc Oxide: Fundamentals, Materials and Device Technology* (WILEY-VCH Verlag GmbH & Co. KGaA, Weinheim)
[26] Jagadish C and Pearton S J 2006 *Zinc Oxide Bulk, Thin Films and Nanostructures: Processing, Properties and Application* (Elsevier Ltd)
[27] Kandjani A E, Shokuhfar A, Tabriz M F , Arefian N A and Vaezi M R 2009 *J. Optel & Adv. Mat*. **11** 289 – 295
[28] van Dijken A, Meulenkamp E A, Vanmaekelbergh D and Meijerink A 2007 *J. Lumin.* **87 – 89** 454